ISSN1027-5495. Functional Materials, 30, No.4 (2023), p. 533-540
doi:http://dx.doi.org/10.15407/fm30.04.533

Composite material "aluminum dodecaboride α-AlB_{12} – fluorinated polyamide": synthesis and properties

V.E.Sheludko[1], V.B.Muratov[1], V.V.Kremenitsky[2], A.V.Pavliuk[3], V.A.Povazhnyi[3], Yu.I.Bogomolov[3]

[1] I.N. Frantsevich Institute for Problems of Materials Science, National Academy of Sciences of Ukraine, 3 Krzhyzhanovsky Str., 03142 Kyiv, Ukraine
[2]Technical Center, National Academy of Sciences of Ukraine, 13 Pokrovskaya Str., 04070 Kyiv, Ukraine
[3]V.P. Kukhar Institute of Bioorganic Chemistry and Petrochemistry, National Academy of Sciences of Ukraine, 50 Kharkovskoe Shausse, 02160 Kyiv, Ukraine

Received August 2,2023

In the article, some properties of composites based on fluorinated aromatic polyamide (polymer matrix) and highly dispersed refractory filler – aluminum dodecaboride α-AlB_{12} are investigated. Fluorinated polyamide was synthesized by low temperature polycondensation in amide solvents. Cross-linked compositions were obtained by high-temperature treatment of a mixture of polyamide, epoxy oligomer, and aluminum dodecaboride (200 °C, 2 h). The particle sizes of aluminum dodecaboride are analyzed by drawing the necessary cross-sections on 2D-images of the surface topography obtained by AFM. The thermal-oxidative stability of aluminum dodecaboride powder and film compositions was studied, and the activation energy of thermal destruction E_a was calculated. To determine the differences in the relief of cross-linked and non-cross-linked samples, the surfaces of the film composites were scanned using AFM. The microhardness of surfaces in cross-linked systems was established to increase significantly with an increase in the content of aluminum dodecaboride, they are also characterized by an increased temperature of deformation strength (up to 300-325 °C). The features of the change in the friction coefficient of the synthesized compositions depending on the material of the counterbody are studied. It is shown that when using synthesized compositions as a counterbody, the friction coefficient decreases by an order of magnitude (f = 0.017-0.059).

Keywords: aluminum dodecaboride, fluorinated polyamide, thermal-oxidative stability, microhardness, friction factor

Композиційний матеріал "додекаборид алюмінію α-AlB_{12} – фторований поліамід": синтез та властивості. *В.Є.Шелудько, В.Б.Муратов, В.В.Кременицький, А.В.Павлюк, В.А.Поважний, Ю.І.Богомолов.*

У статті досліджено деякі властивості композитів на основі фторованого ароматичного поліаміду (полімерна матриця) та тугоплавкого високодисперсного наповнювача – додекабориду алюмінію α-AlB_{12}. Фторований поліамід було синтезовано низькотемпературною поліконденсацією у амідних розчинниках. Зшиті композиції отримані високотемпературною обробкою суміші поліаміду, епоксидного олігомеру та додекабориду алюмінію (200 °C, 2 год). Проаналізовано розміри частинок додекабориду алюмінію шляхом проведення необхідних перерізів на 2D-зображеннях топографії поверхні, отриманих на АСМ. Вивчено

термоокиснювальну стабільність порошку додекабориду алюмінію та плівкових композицій і розраховано енергію активації термодеструкції E_a. Проведено сканування поверхонь плівкових композитів на АСМ з метою визначення відмінностей рельєфу у зшитих та незшитих зразках. Встановлено, що мікротвердість поверхонь у зшитих системах значно зростає із підвищенням вмісту додекабориду алюмінію, також для них характерна підвищена температура деформаційної міцності (до 300-325 °С). Вивчено особливості зміни коефіцієнту тертя синтезованих композицій залежно від матеріалу контртіла. Показано, що при використанні в якості контртіла синтезованих композицій, коефіцієнт тертя зменшується на порядок (f = 0,017-0,059).

1. Introduction

Due to valuable technical properties (high T_m, hardness, fracture strength, chemical stability, high electrical resistance, large thermal-neutron capture cross-section, etc.) borides are not only of independent interest, but are also used to modify the properties of materials in various functional applications [1, 2]. In this regard, it is reasonable to consider the use of borides in polymer materials science.

To increase the thermal conductivity and mechanical strength of polyurethane-epoxy compositions, polyamides, polyimides, silicone and methacrylate materials, hexagonal boron nitride h-BN, as well as titanium diboride TiB_2, and zirconium diboride ZrB_2 were used [3-6]. The amount of introduced boride modifiers ranged from 3 to 5 wt. %, and, in the case of the polyimide-BN system, the content of the latter reached 30 wt. %. The nanocomposite "photoactive polyimide-30 wt. % BN" has excellent thermal properties: glass transition temperature T_g = 360 °C, temperature of the beginning of thermal destruction > 460 °C, and thermal conductivity λ = 0.47 W/m·K. An increase in compressive strength characteristics (~ 40 %) and an increase in thermal conductivity by ~ 8 % compared to the original polyurethane matrix were noted [7].

To modify epoxy compositions, both individual borides and their combinations with oxides (Al_2O_3) or carbides (B_4C) were used. In this case, thermal conductivity increases; thermomechanical behavior and energy intensity of dielectric epoxy resins are improved (~ in 19 times [8-10]).

The effect of borides on the properties of polymerization plastics such as polyvinylidene-TiB_2, polyethylene-TiB_2, -ZrB_2, -NbB_2, polypropylene-BN, polytetrafluoroethylene-TiB_2, -BN was studied. Modification of this type contributes to an increase in T_g, expansion of the temperature range of thermal destruction, an increase in thermal conductivity, electrical insulating, mechanical properties, and high electrical erosion resistance [11-15].

In [16], a synergistic effect was studied as a result of hybrid filling of polytetrafluoroethylene with a system of 7 wt. % ZnO + 23 wt. % BN, which led to a minimum wear rate (up to 1.1·10^{-5} mm^3/N·m) during friction, and an increase in thermal conductivity. It is interesting to note the difference in the method of filling polytetrafluoroethylene with BN and TiB_2 particles. To introduce BN particles (3-5 μm) into polytetrafluoroethylene, the components were mixed under pressure P = 25 MPa, followed by sintering at 380°C for 4 hours. In contrast to this method, a method of mechanical activation processing of ultrafine powder and polytetrafluoroethylene filler has been proposed. This makes it possible to encapsulate the filler in a fluoropolymer shell and then apply it to the substrate using gas dynamic sputtering at room temperature [17].

Among the numerous groups of borides, aluminum borides stand out in terms of their properties. Possessing high hardness, T_m, chemical stability, fracture strength, and the ability to absorb neutrons at low densities, they are increasingly used in practice, for example, as abrasive materials, ceramics, semiconductors, high-value resistors with a low TCR value, as well as in the military field [1, 5]. With an increase in the number of boron atoms, the latter are grouped into icosahedrons and polyhedrons linked by individual boron atoms. Due to the structure, the number of boron atoms bonded to each other increases, thereby increasing the proportion of the covalent component of the bond, which leads to an increase in the physicochemical characteristics of α-AlB_{12}, for example, T_m up to 2436 K (argon). A decrease in the proportion of the covalent component, for example, in AlB_2, reduces T_m to 1928 K. The properties of α-AlB_{12} predetermined its use in heat-resistant ceramic materials. To a lesser extent, α-AlB_{12} is known as filler in polymeric materials. Nevertheless, there is information about the fabrication of collimators for neutron spectrometers, based on α-AlB_{12} and a phenol-formaldehyde binder [1]. A very important property of α-AlB_{12}

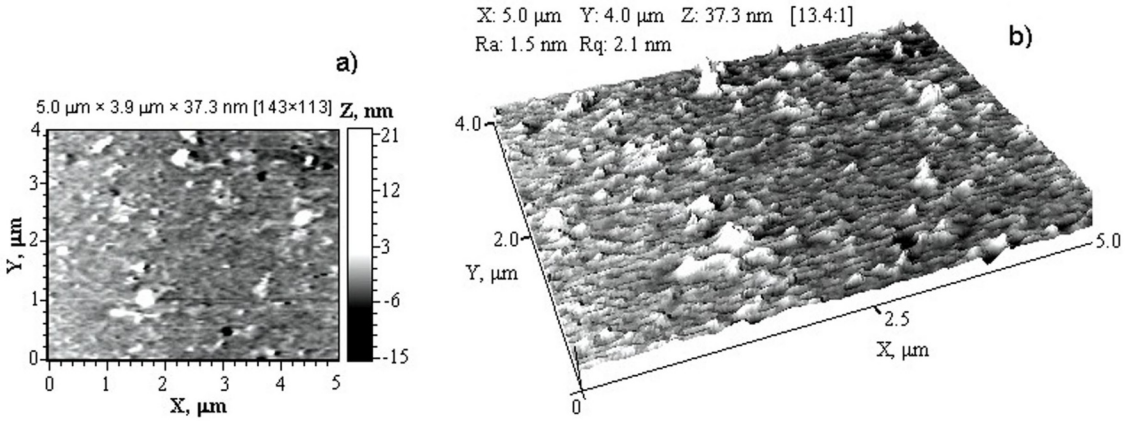

Fig. 1 – 2D- (a) и 3D- (b) images of surface topography formed by particles α-AlB_{12}

is its high energy capacity exceeding this characteristic for other aluminum borides. This value is 135.9 J/lit [18].

The high value of the heat of combustion and the best reactivity in the combustion process predetermined the use of α-AlB_{12} in military applications as a promising component of solid composite rocket fuels; especially since methods have now been developed for producing aluminum borides in quantities of tens of kilograms, in particular the method of arc plasma recondensation [19-20].

So, an analysis of the literature indicates that aluminum dodecaboride α-AlB_{12} is a promising material for use in various industries. However, its compositions with heat-resistant polymers are practically not studied. Since these composites were obtained for the first time, the article evaluates the influence of α-AlB_{12} on the thermal characteristics, microhardness, deformation heat-resistance, structure of film composites, changes in the surface relief; the fundamental possibility of their use in tribological applications was also assessed.

The aim of the work was to synthesize the composites based on a fluorine-containing aromatic polyamide and refractory α-AlB_{12} and study their physical-chemical characteristics.

2. Experimental

Aluminum dodecaboride powder α-AlB_{12} was synthesized by vacuum heat treatment of a mixture of the powders of aluminum and hexagonal boron nitride according to the reaction $12BN + 13Al \rightarrow AlB_{12} + 12AlN$ [21]. The average particle size of the α-AlB_{12} powder is about 120÷150 nm, T_m = 2070 °C.

The polymer matrix used was a fluorine-containing aromatic polyamide (PA) – poly-1-tetrafluorethoxy-2,4-phenylenisophthalamide [22], which is Phenylone™ modified with a tetrafluoroethoxy group, the structural formula and some properties of which are given in [23].

Film composite materials (CM) were obtained from a polymer solution to which α-AlB_{12} powder (0.5, 1, 5, and 20 wt. % of polyamide weight) was added. Cross-linked samples were obtained by adding an epoxy component (ED-20 epoxy resin, GOST 10587-84) followed by forming on a glass or fluoroplastic substrate at T = 80 °C. The formed samples were annealed at T = 200 °C for 2 hours at a fixed film length. The thickness of the film composite is ~70-100 μm. Thermomechanical studies were carried out at a load of 0.1 MPa and a heating rate of 6 °C/min.

The microhardness of the films was measured on a PMT-3 microhardness tester at a load P = 0.5-1.5 N. Tribological studies were carried out on a Tribotest friction machine according to the "plane-plane" scheme in the mode: P = 0.5 MPa, V = 0.8 m/s, friction path S = 3 km. Hardened Steel 45 (HRC 48-52) was used as a counterbody.

The study of the processes of oxidation of α-AlB_{12} and thermal-oxidative destruction of CM was carried out on a simultaneous TG-DSC/DTA analyzer STA PT1600 (Linseis Messgeraete GmbH, Selb, Germany) and on a derivatograph (MOM, Hungary) at a heating rate of 10 °C/min.

The topography of the film surface was studied on an NT-206 atomic force microscope (ODO "Mikrotestmashines", Gomel, Republic of Belarus) using a CSC37 probe (MikroMasch OÜ, Tallinn, Estonia) with a cantilever stiffness of 0.3-0.6 N/m. The scanning step is 0.3 nm; the scanning speed is 10 μm/s in the X-Y plane. The structure of the films was studied

using a JEOL JSM-6490 LV SEM equipped with an energy-dispersive X-ray microanalysis system (Oxford Instruments plc.).

3. Results and discussion

Fig. 1a shows a 2D-image (topography) of the surface formed by α-AlB_{12} particles on a fused quartz substrate, and Fig. 1b shows a 3D-image of this area.

The surface topography is determined by the presence of small particles and their aggregates. The surface roughness in this area is R_a = 1.5 nm (Fig. 1b), and the range of hollows and heights is -7.2 ÷ +6.7 nm. To determine the size of the particles, sections were made over small and large formations and their profiles were plotted. Their analysis indicates that the heights of the relief formed by nanoparticles are 1.8; 2.2; 2.5; 4.3; 5.2 nm. The heights formed by large particles are within 14.6; 25; 3.7; 5; 15.6 nm, i.e. larger aggregates are also concentrated in this area of the surface.

To evaluate the thermal-oxidative stability of α-AlB_{12}, a thermogravimetric analysis combined with differential scanning calorimetry was carried out (Fig. 2).

The temperature of the beginning of intensive oxidation (weight gain), determined by the tangents to the TGA curve, is 670 °C. It practically coincides with the temperature of the beginning of heat generation. With a subsequent increase in temperature (680-690 °C), the heat generation increases to a maximum and the weight gain sharply increases up to a temperature of ~740 °C. After that, the weight gain curve reaches a flat section, the weight gain rate decreases, and at 1200 °C, the weight gain is maximum – 22.8 mg, i.e. is ~215.09 % (the initial mass of the sample is 10.6 mg). According to TGA (MOM derivatograph), the weight gain was ~214.12 %, and the temperature of the maximum weight gain rate was 757 °C. Another feature of oxidation under these conditions is that after reaching 1200 °C and turning off the device, with decreasing temperature, the gain decreases to 590 °C, after which it begins to slightly increase, despite the decrease in temperature. This can be obviously explained by the fact that in the temperature range from 1200 to 590 °C, boron oxides are evaporated for 30 min [24] which leads, firstly, to a decrease in weight gain, and, secondly, to the appearance of open surface areas available for further oxidation and, as a consequence, to some increase in weight gain.

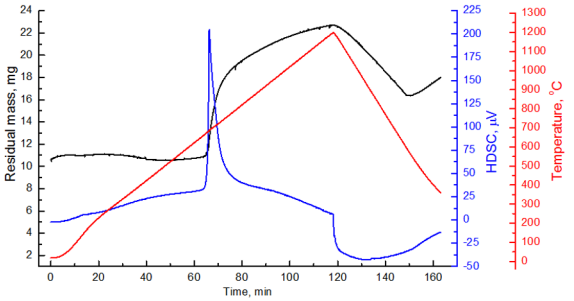

Fig. 2. TGA and DSC α-AlB_{12} on air

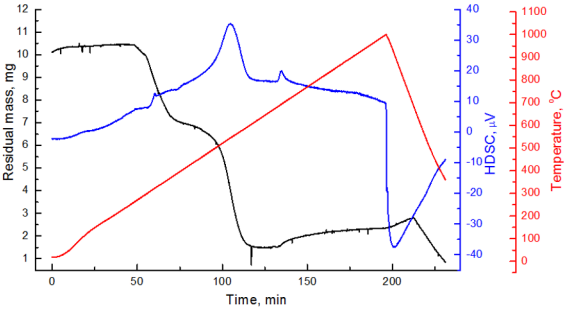

Fig. 3. TGA and DSC for CM with 5 wt. % α-AlB_{12} on air

According to the literature data [19], the temperature of the beginning of intense oxidation of α-AlB_{12} depends on the heating rate and comes to 712, 731, 760, and 792 °C at heating rates of 2, 4, 10, and 20 °C/min, respectively. The temperature of the maximum rate of the process (757 °C) obtained in our experiments at a heating rate of 10 °C/min coincides with the published data.

Three stages of the CM thermal oxidation process are revealed by TGA. The first two relate to the destruction of the polymer matrix with a corresponding weight loss, and the third characterizes the oxidation of the boride remaining after the destruction of the polymer with a corresponding weight gain up to a temperature of 1200 °C. A characteristic feature of the thermal-oxidative destruction of these samples is that at, for example, 5 wt. % α-AlB_{12} introduced into the initial polyamide film, the process of stopping weight loss ends at 590 °C; and the weight gain during boride oxidation begins after 20 min at 690 °C. A similar process occurs in a cross-linked system with 5 wt. % α-AlB_{12}, but over a shorter period of time (13.6 min): the destruction of the polymer ends at 600 °C, and the weight gain begins at 680 °C (Fig. 3).

A somewhat different process occurs with the introduction of 0.5 wt. % α-AlB_{12}. After the polymer destruction at 720 °C, a period of mass stabilization begins for ~30 min; and only when

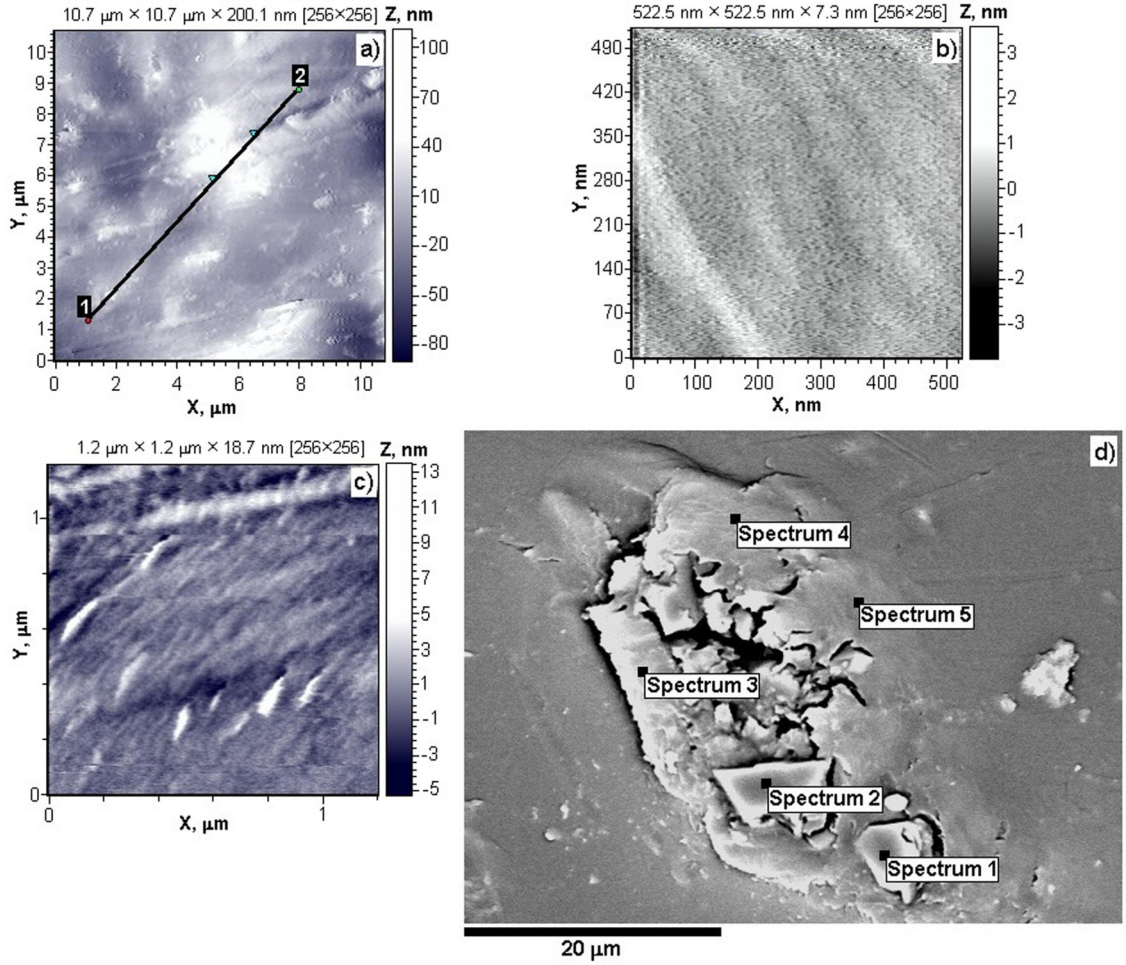

Fig. 4. 2D image of the surface relief of film CMs (uncross-linked composite: a – top; b – bottom), c – cross-linked composite, top, d – aggregate surface structure with microanalysis data (Table 2)

the temperature reaches 1000 °C, the oxidation of borides begins, accompanied by an increase in weight. The activation energies E_a of the thermal destruction of the polymer part of the composites at stages I and II are given in Table 1.

To study the effect of α-AlB_{12} on the surface topography of film CMs, atomic force microscopy was used for a sample of the composition "fluorinated PA-5 wt. % α-AlB_{12}".

Fig. 4a shows a 2D-image of the upper surface of the film CM where large aggregates formed. The difference between heights and hollows is from -63.7 to +73.6 nm in this case. The analysis of the cross-section profile showed that the particle heights are from 34 to 40.2 nm with a width of ~20 μm. The surface roughness R_a = 17.3 nm. In contrast to the upper surface, the relief of the film from the side of the substrate (Fig. 4b) is uniform with a small height difference from -1.3 to +1.2 nm, at R_a = 0.3 nm. The heights of the relief formed by α-AlB_{12} nanoparticles are 0.8; 0.5; 0.7; 1 nm.

Table 1. Activation energies of thermal-oxidative destruction of composites

Wt.% of α-AlB_{12}	Activation energy, E_a, kcal/mol	
	I stage	II stage
0.5	83.98	13.26
5	70.05	64.14
5 (cross-linked)	71.61	45.6

The relief of the film "fluorinated PA cured with ED-20 – α-AlB_{12}" differs from that of the uncured sample. This surface is characterized by the presence of ordered regions with almost parallel packing and elongated individual aggregates (Fig. 4c) with a length of 128-174.5 nm and a height of 1.8-12.0 nm. The total surface roughness R_a = 1.0 nm. The surface relief from the side of the substrate is a conglomerate of fibrous formations with a height of 12.1 to 20.8

Table 2 - Chemical composition of film CM (Fig. 4d)

Spectrum	Element, wt.%					Total
	B	Al	C	O	F	
1	89.63	10.37	-	-	-	100,00
2	90.94	9.96	-	-	-	100,00
3	-	0.33	76.70	13.69	9.28	100,00
4	-	-	74.30	13.57	12.13	100,00
5		1.29	75.01	13.70	10.01	100,00

nm, a width of 66.1 to 119.1 nm, with a total roughness R_a = 10.1 nm.

Fig. 4d shows a fragment of the surface image in secondary electrons with indication of the microanalysis sites (spectra 1-4, Table 2).

The microhardness of film CMs was estimated by comparing the values at different loads on the indenter. With the introduction of 1 wt. % α-AlB_{12} during the formation of a polyamide film, the microhardness of the samples is in the range of 226.63-238.2 MPa. An increase in the content of α-AlB_{12} to 5 wt. % slightly increases the microhardness (up to 291.25-298.02 MPa). This value corresponds to the microhardness of pressed samples of Phenylone™ aromatic polyamide, which is 274.58-294.19 MPa [25]. Studies have shown that the microhardness in cross-linked systems increases significantly. For example, the surface microhardness of the cross-linked sample containing 1 wt. % α-AlB_{12} is ~6.82 GPa, which is ~10 times higher than this value for a non-cross-linked one. There is an even greater difference in the microhardness of the non-cross-linked and cross-linked samples containing 5 wt. % α-AlB_{12}: 292.53 MPa and 11.26 GPa (~38 times higher). Thus, it is possible to regulate the microhardness of CM depending on the content of α-AlB_{12}.

To evaluate the deformation heat-resistance of film samples, thermomechanical studies were carried out. One of the methods of increasing heat-resistance is to develop cross-linked systems. In particular, it has been found that cross-linked polyamides can be obtained by modification with epoxy resins. In this case, as a result of the interaction of the amide group of the polyamide with the epoxy group, a cross-linked polymer is formed. This leads to an increase in heat-resistance compared to the unmodified sample. At that, the initial polyamide loses solubility in amide solvents (for example, the value of the gel fraction is 97-98 % with the introduction of 15 wt. % ED-20 epoxy resin). By adjusting the amount of modifier introduced followed by high-temperature curing, it is possible to obtain compositions with varying degrees of curing. The temperature of the beginning of deformation under load for the initial fluorinated polyamide is 238-240 °C [26]. Fig. 5 shows thermomechanical curves for film compositions with different contents of α-AlB_{12}. These data indicate that after curing, the temperature range for the onset of deformation of the composites shifts to higher values (300-325°C).

Table 3 - Friction coefficient f of the developed film CMs

Modifier, wt.%	Friction pair	
	CM-Steel 45	CM-CM
	f	*f*
α-AlB_{12}, 1	0.240	0.033
α-AlB_{12}, 5	0.196	0.022
α-AlB_{12}, 20	0.251	0.044
Composite without addition of borides	0.28	0.017
α-AlB_{12} / AlN, (20/20)	0.26	0.059
AlN, 20	0.24	0.022

Taking into account the aforementioned high physicochemical characteristics of α-AlB_{12}, it can be assumed that the latter can be effective filler in compositions for heat-loaded assemblies, in particular, friction pairs. To find out the possibility of using polyamide-epoxy matrices with α-AlB_{12} as filler, some of their tribological characteristics were studied.

Thus, the compositions were developed in which, in addition to the binder and α-AlB_{12}, the following were introduced: a tribo-polymer-forming additive, antifriction filler, antioxidants, and a solvent system. The resulting suspension containing α-AlB_{12} (1, 5, and 20 wt. %) was applied to bronze bushings BrOTsS5-5-5 (20 mm in diameter) and cured at T = 200 °C.

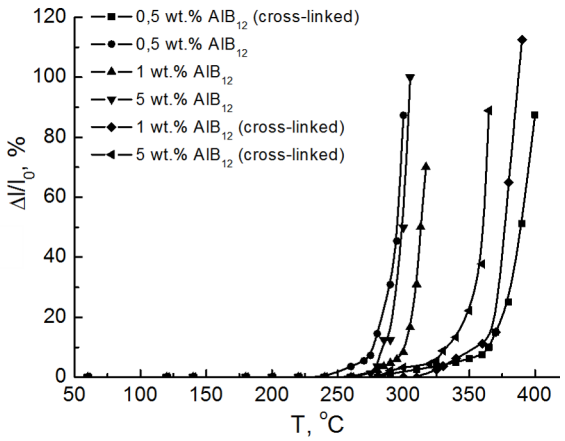

Fig. 5. Thermomechanical curves of film CMs

Table 3 shows the main data on the tribology of the composites. It should be noted that the non-fluorinated aromatic polyamide Phenylone™ has a high friction coefficient f = 0.4-0.5 under dry friction, which leads to an increased temperature in the friction zone, and with increasing load – to increased wear. Therefore, graphite, BN, F-4 fluoroplastic, and other antifriction additives are introduced to reduce the friction coefficient. In our case, the composition includes α-AlB_{12}. Aluminum borides are known as abrasives, especially in combination with SiB_6, to work at high speeds [1]. Therefore, it was to be expected that the developed compositions would be able to work as friction materials. Tests have shown that the value of the coefficient of dry friction for Steel 45 is from 0.19 to 0.33 with virtually no weight wear.

However, α-AlB_{12} is characterized by low thermal conductivity (λ = 3.1-4.3 W/m·K), which determines the intensity of heat transfer. AlN is of interest as a modifier having a high thermal conductivity (up to 200 W/m·K), a low thermal expansion coefficient of $4.8 \cdot 10^{-6}$ $^{o}C^{-1}$, and high thermal-oxidative stability (AlN oxidation starts at 700-800 °C).

The introduction of AlN (20 wt. %) into the composition and in the form of a binary filler with α-AlB_{12} (20 wt. % / 20 wt. %) slightly reduces f compared to the system without boride (0.26-0.29), however, these compositions can be used to work as friction materials.

It was of interest to study some tribological characteristics of the developed CMs in a friction pair with the same counterbody. Similar friction pairs have been tested on the example of sintered materials and even put into practice. There is information in the literature about the use of friction pairs in the braking devices of the Concord aircraft, in which both linking elements were made of sintered materials. In some properties (torque, service life, smoothness of moving out), such units are superior for brakes in which alloy steel was chosen as the counterbody [27]. The paper [28] presents the data on tribological studies of ceramic CMs, such as SiC-Al_2O_3 and SiC-Al_2O_3-ZrO_2 in a ceramic-ceramic friction pair. A decrease in the wear intensity was achieved in comparison with the steel counterbody (I = 4.7 μm/km). It has been established that with an increase in the duration of the charge milling, the wear resistance of ceramic CMs increases by 7 times.

The tribological properties of polymer-polymer friction pairs were studied in [29], where the counterbody was polycarbonate (PC), and polyamide (PA6), polytetrafluoroethylene (PTFE), and the polypropylene (PP) were conjugate polymers. The friction coefficient f = 0.084-0.094 was recorded in the friction pairs "PC-PTFE", "PC-PA6". In the "PC-PTFE" friction pair, the friction coefficient decreased from 0.25 to 0.07 after 30 min of sliding at P = 50 N.

In our case, we tested friction pairs in which the counterbody was a similar CM based on α-AlB_{12}. Data in Table 3 indicate that during the operation of such friction pairs, in which both elements are made of similarly developed CMs, the friction coefficient decreases by an order of magnitude and ranges from 0.017 to 0.059 with virtually no weight wear. Thus, this example shows the advisability of such an approach for practical use.

4. Conclusions

For the first time, CMs based on a fluorine-containing polyamide-epoxy matrix and aluminum dodecaboride α-AlB_{12} were developed and some of their physicochemical properties were studied.

The III-stage process of thermal oxidation has been established. The stages I and II relate to the thermal-oxidative destruction of the polymer part of the CM, and the third characterizes the oxidation of α-AlB_{12} with a corresponding weight gain. The values of the activation energy E_a of the process range from 70.05 to 84 kcal/mol and from 13.26 to 64 kcal/mol at the stages I and II, respectively.

Introduction from 1 to 5 wt. % α-AlB_{12} increases the value of microhardness of cross-linked samples from 10 to 38 times. At the same time, their temperature range of deformation heat-resistance is 300-325 °C.

For friction on Steel 45, the value of *f* is in the range from 0.19 to 0.33, which corresponds to the work of friction pairs. In the CM-CM friction pair, the value of *f* decreases by an order of magnitude and amounts to 0.017-0.059, which indicates the possible use of such systems for antifriction pairs.

References

1. P.S.Kisly, V.A.Neronov, T.A.Prikhna et al, Aluminum Borides, Nauk. Dumka, Kiev (1990) [in Russian].
2. J.L.Colon Quintana, S.Soto Medina, M.Hernandez, *Adv. Mater. Sci Eng.*, ArticleID 2975234, (2018). DOI: doi.org/10.1155/2018/2975234.
3. N.A.Bratasyuk, N.N.Saprykina, V.V.Zuev. *Mat. Chem. Phys.*, **277**, 125514 (2022). DOI: doi.org/10.1016/j.matchemphys.2021.125514.
4. J.Joy, E.George, P.Haritha et al., *J. Polym. Sci.*, **58**, 3115 (2020). DOI: doi.org/10.1002/pol.20200507.
5. M.L.Whittaker, Synthesis, Characterization and Energetic Performance of Metal Boride Compounds for Insensitive Energetic Materials, The Univ. of Utah, College of Eng., Master Thesis, 2012.
6. T.-L.Li, S.L.-C.Hsu, *J. Appl. Polym. Sci.*, **121**, 916 (2011). DOI: doi.org/10.1002/app.33631.
7. M.Sadej, L.Gierz, M.Naumowicz, *Polimery*, **64**, 591 (2019). DOI: dx.doi.org/10.14314/polimery.2019.9.3.
8. Ye and Z.Yu., *J. Polym. Eng.*, 2019, **39**, 508 (2019). DOI: doi.org/10.1515/polyeng-2018-0375.
9. Z.-Q.Yu, Y.Wu, B.Wei et al., *Mat. Chem. Phys.*, **164**, 214 (2015). DOI: doi.org/10.1016/j.matchemphys.2015.08.049.
10. A-K.A.Kallinikou, Th.G.Velmachos and G.C.Psarras, in: Proc. 18th Europ. Conf. on Composite Materials (ECCM18), Athens, Greece (2018), Poster P_2.46.
11. A.Joseph, G.M.Joshi, *J. Mat. Sci: Mat. Electron.*, **29**, 4749 (2017). DOI: doi.org/10.1007/s10854-017-8431-z.
12. T.R.Shrout, D.Moffatt, W.Huebner, *J. Mat. Sci.*, **26**, 145 (1991).
13. G.B.Vaggar, V.B.Sirimani, D.P.Sataraddi, *Int. J. Eng. Res. Technol.*, **10**, ArticleID IJERTV10IS080008 (2021). DOI: doi.org/10.17577/IJERTV10IS080008.
14. W.Zhou, S.Qi, H.Li et al., *Thermochim. Acta*, **452**, 36 (2007). DOI: doi.org/10.1016/j.tca.2006.10.018.
15. B.C.D.Luan, J.Huang, J.Zhang, *J. Appl. Polym. Sci.*, ArticleID 42302 (2015). DOI: doi.org/10.1002/app.42302.
16. X.Q.Pei and K.Friedrich, Friction and Wear of Polymer Composites, in *Reference Module in Materials Science and Materials Engineering*, Elsevier, Amsterdam, The Netherlands (2016). DOI: doi.org/10.1016/B978-0-12-803581-8.03074-5.
17. V.M.Buznik, *Russian Nanotechnologies*, **4**, 35 (2009) [in Russian].
18. V.N.Bakulin, N.F.Dubovkin, V.N.Kotova et al., Energy-intensive Fuels for Aircraft and Rocket Engines, Fizmatlit, Moscow (2009) [in Russian].
19. A.G.Korotkikh, K.V.Slyusarsky, I.V.Sorokin, *Chem. Phys. Mesoscopy*, **22**, 164 (2020). DOI: doi.org/10.15350/17270529.2020.2.16 [in Russian].
20. Sh.L.Guseinov, S.G.Fedorov, A.Yu.Tuzov, *Nanotechnologies in Russia*, **10**, 420 (2015). DOI: doi.org/ 10.1134/S199507801503009X.
21 UA Patent 107193 (2016).
22 B.F.Malichenko and O.N.Tsipina, *Vysokomolek. Soed.*, **B11**, 361 (1979) [in Russian].
23 A.V.Paustovskii, B.M.Rud', V.E.Shelud'ko et al., *Powder Metall. Met. Ceram.* **55**, 437 (2016). DOI: doi.org/10.1007/s11106-016-9824-x.
24 G.V.Samsonov, T.I.Serebryakova, V.A.Neronov, Borides, Atomizdat, Moscow (1975) [in Russian].
25 L.B.Sokolov, V.D.Gerasimov, V.M.Savinov et al., Thermostable Aromatic Polyamides, Khimiya, Moscow (1975) [in Russian].
26 O.N.Tsipina, Ye.V.Sheludko, *Lakokrasochnyye Materialy i ih Primeneniye*, **2**, 15 (1990) [in Russian].
27 I.M.Fedorchenko, V.M.Kryachek, I.I.Panaiotti, Modern Frictional Materials, Nauk. Dumka, Kiev (1975) [in Russian].
28 O.P.Umanskii, A.G.Dovgal, V.L.Syrovatka et al., Silicon Carbide-based Composition Materials for Compacted Products and Gas-Thermal Coatings, Nauk. Dumka, Kiev (2022) [in Ukrainian].
29 Wagih W.Marzouk, Mustafa A.Abdel-Rahman, *Tribologia*, **5**, 97 (2012).